

Supplementary information

Exploring the interaction of decavanadate with methylene blue, toluidine blue and rhodamine B

Juliana M. Missina^{1*}, Heloísa de S. Camilo¹, Rúbia C. R. Bottini¹, Isabela Passadore de Souza e Silva¹, Lucas G. Fachini¹, Patrizia Rossi², Paola Paoli², Eduardo L. de Sá¹ and Giovana G. Nunes^{1*}

¹Departamento de Química, Universidade Federal do Paraná, Curitiba-PR, Brazil

²Dipartimento di Ingegneria Industriale, Università degli Studi di Firenze, Firenze, Italy

	CONTENTS	page
Table S1.	Bond lengths (Å) and angles (°) for the V ₁₀ anion in 2,3-ampV₁₀ and MBV₁₀	2
Table S2.	Decavanadate salts containing aminopyridines as counterions found in the CCDC database	4
Table S3.	Tentative assignments for the IR spectrum of (2,3-ampH) ₆ [V ₁₀ O ₂₈]·4H ₂ O (2,3-ampV₁₀)	4
Table S4.	Tentative assignments for the IR spectra registered for MBV₁₀ and TBV₁₀	5
Table S5.	Final discoloration values of MB solution at 10.0 mg L ⁻¹ and TB at 10.0 mg L ⁻¹ bleached by 2,3-ampV₁₀	5
Figure S1.	Calculated and experimental PXRD patterns of 2,3-ampV₁₀ .	6
Figure S2.	A) ORTEP view of the asymmetric unit of 2,3-ampV₁₀ . B) Chain formed by the 2,3-ampH ⁺ cation and V ₁₀ anions interactions in 2,3-ampV₁₀ . C) 2,3-ampH ⁺ cation and V ₁₀ anions network.	7
Figure S3.	Calculated and experimental PXRD patterns of MBV₁₀ .	8
Figure S4.	PXRD pattern of ATV₁₀ .	8
Figure S5.	IR spectrum of (2,3-ampH) ₆ [V ₁₀ O ₂₈]·4H ₂ O (2,3-ampV₁₀).	9
Figure S6.	IR spectrum recorded for the solids isolated from MB bleaching reactions with 2,3-ampV₁₀ .	9
Figure S7.	IR spectrum recorded for the solids isolated from TB bleaching reactions with 2,3-ampV₁₀ .	10
Figure S8.	ORTEP view of the asymmetric unit of MBV₁₀ . Ellipsoid probability 30%.	10
Figure S9.	Electronic spectra registered for the supernatants of the bleaching reactions using 10 mg of 2,3-ampV₁₀ in 10 mg L ⁻¹ aqueous solution of RB in time.	11
Figure S10.	ESI-MS scan of MB in positive mode: A) before and B) after the reaction with 10 mg of 2,3-ampV ₁₀ .	12
Figure S11.	ESI-MS scan of TB (10 mg L ⁻¹) in positive mode: A) before and B) after the reaction with 10 mg 2,3-ampV ₁₀ .	13
Figure S12.	ESI-MS scan of 2-amino-3-methylpyridine in methanol in positive mode.	14

Table S1. Bond lengths (Å) and angles (°) for the V₁₀ anion in **2,3-ampV₁₀** and **MBV₁₀**

2,3-ampV₁₀		MBV₁₀
<i>Bonds (Å)</i>		
V1-O1	1.609(3)	1.595(6)
V1-O2	1.901(2)	2.048(5)
V1-O3	2.064(2)	1.846(6)
V1-O4	1.864(2)	1.827(6)
V1-O5	1.799(2)	1.910(6)
V1-O14	2.345(2)	2.330(5)
V2-O2	1.784(2)	1.684(5)
V2-O6	1.616(2)	1.676(5)
V2-O7	1.972(2)	2.009(6)
V2-O13	1.860(2)	1.894(6)
V2-O14	2.236(2)	2.106(5)
V3-O3	1.683(2)	1.845(6)
V3-O7	1.926(2)	2.057(5)
V3-O8	1.687(2)	1.597(6)
V3-O9	1.942(2)	1.789(6)
V3-O14	2.098(2)	2.273(6)
V4-O4	1.807(2)	1.833(6)
V4-O9	1.979(2)	1.879(6)
V4-O10	1.615(2)	1.604(5)
V4-O11	1.843(2)	1.892(6)
V4-O14	2.239(2)	2.322(5)
V5-O5	1.846(2)	1.763(5)
V5-O11	1.870(2)	1.882(5)
V5-O12	1.616(2)	1.595(7)
V5-O13	1.859(2)	1.966(5)
V5-O14	2.294(2)	2.274(6)
<i>Angles (°)</i>		

O1-V1-O2	101.7(2)	100.0(3)
O1-V1-O3	100.2(1)	102.3(3)
O1-V1-O4	102.5(1)	104.5(3)
O1-V1-O5	105.3(1)	101.5(3)
O1-V1-O14	173.2(1)	173.2(2)
O2-V1-O3	81.75(9)	84.2(2)
O2-V1-O4	153.2(1)	155.4(2)
O2-V1-O5	91.8(1)	82.3(2)
O2-V1-O14	76.95(9)	73.4(2)
O3-V1-O4	82.72(9)	93.1(2)
O3-V1-O5	154.5(1)	154.4(3)
O3-V1-O14	73.01(8)	78.6(2)
O4-V1-O5	92.9(1)	90.2(3)
O4-V1-O14	77.67(9)	82.1(2)
O5-V1-O14	81.47(9)	76.8(2)
O2-V2-O6	102.7(1)	106.6(3)
O2-V2-O7	92.8(1)	94.2(3)
O2-V2-O13	95.4(1)	99.4(3)
O2-V2-O14	82.20(9)	86.9(2)
O6-V2-O7	100.8(1)	95.2(3)
O6-V2-O13	101.7(1)	99.0(3)
O6-V2-O14	174.8(1)	165.9(2)
O7-V2-O13	153.7(1)	156.6(2)
O7-V2-O14	76.95(8)	79.8(2)
O13-V2-O14	79.49(9)	82.0(2)
O3-V3-O7	97.2(1)	87.9(2)
O3-V3-O8	106.7(1)	102.2(3)
O3-V3-O9	97.7(1)	95.7(2)
O3-V3-O14	87.55(9)	80.1(2)
O7-V3-O8	97.0(1)	99.3(3)
O7-V3-O9	156.48(9)	154.7(2)

O7-V3-O14	81.34(9)	75.0(2)
O8-V3-O9	96.0(1)	104.3(3)
O8-V3-O14	165.71(9)	173.8(3)
O9-V3-O14	81.24(9)	81.0(2)
O4-V4-O9	91.31(9)	91.6(3)
O4-V4-O10	101.9(1)	104.1(3)
O4-V4-O11	95.5(1)	91.5(3)
O4-V4-O14	81.66(9)	82.2(2)
O9-V4-O10	100.1(1)	102.3(3)
O9-V4-O11	154.6(1)	154.9(3)
O9-V4-O14	76.98(8)	77.9(2)
O10-V4-O11	102.4(1)	101.1(3)
O10-V4-O14	175.5(1)	173.6(3)
O11-V4-O14	79.80(9)	77.9(2)
O5-V5-O11	90.4(1)	95.5(3)
O5-V5-O12	103.4(1)	105.0(3)
O5-V5-O13	91.7(1)	93.3(2)
O5-V5-O14	81.96(9)	81.1(2)
O11-V5-O12	101.9(1)	102.5(3)
O11-V5-O13	155.2(1)	152.4(2)
O11-V5-O14	77.81(9)	79.3(2)
O12-V5-O13	101.7(1)	100.4(3)
O12-V5-O14	174.6(1)	173.3(3)
O13-V5-O14	77.97(9)	76.3(2)

Table S2. Decavanadate salts containing aminopyridines as counterions found in the CCDC database

Organic part	Formulation	CCDC# refcode	Ref.
2-aminopyridine	[2-ampH] ₆ [V ₁₀ O ₂₈]·2H ₂ O	DEFPIO, DEFPIO01, DEFPIO02,	1-3
	{[Cu(2-amp) ₂ (H ₂ O) ₂ H ₂ V ₁₀ O ₂₈]}·4H ₂ O	FASBEI	4
	{[Co(3-amp)(H ₂ O) ₅] ₂ [3-ampH] ₂ [V ₁₀ O ₂₈]·6H ₂ O [3-ampH] ₆ [V ₁₀ O ₂₈]·2H ₂ O}	SUDGEG AROYOW	5 6
3- aminopyridine	[4-dmampH] ₄ [H ₂ V ₁₀ O ₂₈]·5H ₂ O*	ROSYEG	7
	[4-ampH] ₁₀ {[Na(H ₂ O) ₆]{[HV ₁₀ O ₂₈]}}[V ₁₀ O ₂₈]·15H ₂ O	SUDGIK	5
	{[4-ampH] ₆ {Co(H ₂ O) ₆] ₃ [V ₁₀ O ₂₈] ₂ ·14H ₂ O [4-ampH] ₁₀ {Zn(H ₂ O) ₆ }][V ₁₀ O ₂₈] ₂ ·10H ₂ O}	SUDGOQ SUDGUW	5
4- aminopyridine	[4-dmampH] ₆ [V ₁₀ O ₂₈]·16H ₂ O	ZADHUK, ZADHUK01	8, 9
	[4-dmampH] ₆ [V ₁₀ O ₂₈]·H ₂ O	XEHZIW	9
	[4-dmampH] ₄ (NH ₄) ₂ [V ₁₀ O ₂₈]·8H ₂ O	WULQIF	10
4- dimethylaminopyridinium	[(C ₇ H ₁₁ N ₂) ₄][Mg(H ₂ O) ₆][O ₂₈ V ₁₀] ₄ H ₂ O	LOPGOQ	11

*dmampH = dimethylaminopyridinium cation

CCDC = Cambridge Crystallographic Data Centre

Table S3. Tentative assignments for the infrared absorption spectrum (cm⁻¹) of (2,3-ampH)₆[V₁₀O₂₈]·4H₂O (**2,3-ampV₁₀**)^{12, 13}

Tentative assignments	2,3-ampV ₁₀
$\nu(O-H)$ and $\nu(N-H)$	3551, 3356 and 3176
$\nu(C-C)_{ring}$, $\delta(N-H)$ or $\delta(O-H)_{water}$	1653
$\nu(C-C)_{ring}$ and $\delta(N-H)$	1566
$\delta(CH_3)$	1470, 1387, 1362 and 1304
$\nu(C=N)$	1252
$\nu(V=O)$	947
$\nu_{as}(V-O)$ $\nu_{sym}(V-O)$ and $\delta(C-H)$	839 and 737
$\delta(V-O-V)$	594 and 453
$\delta(C-N-C)$	538

 ν = stretching, ν_{as} = asymmetric stretching, ν_{sym} = symmetric stretching, and δ = in- or out-of-plane bending

Table S4. Tentative assignments for the IR (cm^{-1}) spectra registered for **MBV₁₀** and **TBV₁₀**¹⁴⁻¹⁷

Assignment	MBV ₁₀	TBV ₁₀
$\nu(\text{O-H})$ and $\nu(\text{N-H})$	3450 and 3348	3314 and 3188
$\delta(\text{N-H})$	-	1599
$\nu(\text{C=N}), \nu(\text{C-C})$	1599, 1221	1649
$\nu(\text{C=S}^+)$	1489	1486
$\delta(\text{C-H})$	1441, 1392, 1252 and 1178	1323, 1487
$\delta(\text{C-N})$	1153	1385
$\nu(\text{C-S-C})$	1040	1025
$\nu(\text{V=O})$	964	959
$\nu_{\text{as}}(\text{V-O})$ and $\nu_{\text{sim}}(\text{V-O})$	831 and 760	827 and 744
$\delta(\text{V-O-V})$	607	663

ν = stretching, ν_{as} = asymmetric stretching, ν_{sim} = symmetric stretching e δ = in-plane angular deformation

Table S5. Final discoloration values of MB solution at 10.0 mg L⁻¹ and TB at 10.0 mg L⁻¹ bleached by **2,3-AmpV₁₀** represented by arithmetic mean (%) ± standard deviation (SD) in the different reaction conditions

Reaction condition	Reaction time (min)	MB* bleaching (%) ± SD	TB * bleaching (%) ± SD
<i>General investigation (pH 6)</i>			
10.0 mg of 2,3-AmpV₁₀ + AM _(aq) a 10.0 mg L ⁻¹	15	89.88±0.57	70.27±0.79
<i>Effect of 2,3-AmpV₁₀ amount (pH 6)</i>			
16 mg of 2,3-AmpV₁₀ + dye solution	15	NA	77.28±1.17
4.0 mg of 2,3-AmpV₁₀ + dye solution	15	86.54±1.48	49.50±4.46
2.0 mg of 2,3-AmpV₁₀ + dye solution	15	82.67±0.24	NA
1.0 mg of 2,3-AmpV₁₀ + dye solution	15	32.10±2.05	NA
<i>Presence of peroxide</i>			
10.0 mg of 2,3-AmpV₁₀ + dye solution + 1.0 mL de H ₂ O ₂ 35%	10	90.50±0.64	NA
<i>pH 3</i>			
10.0 mg of 2,3-AmpV₁₀ + dye solution, pH 3	15	93.18±0.73	83.57±1.10

NA = Data not available,

* monitored absorption wavelength for MB = 664 nm and for TB = 630 nm

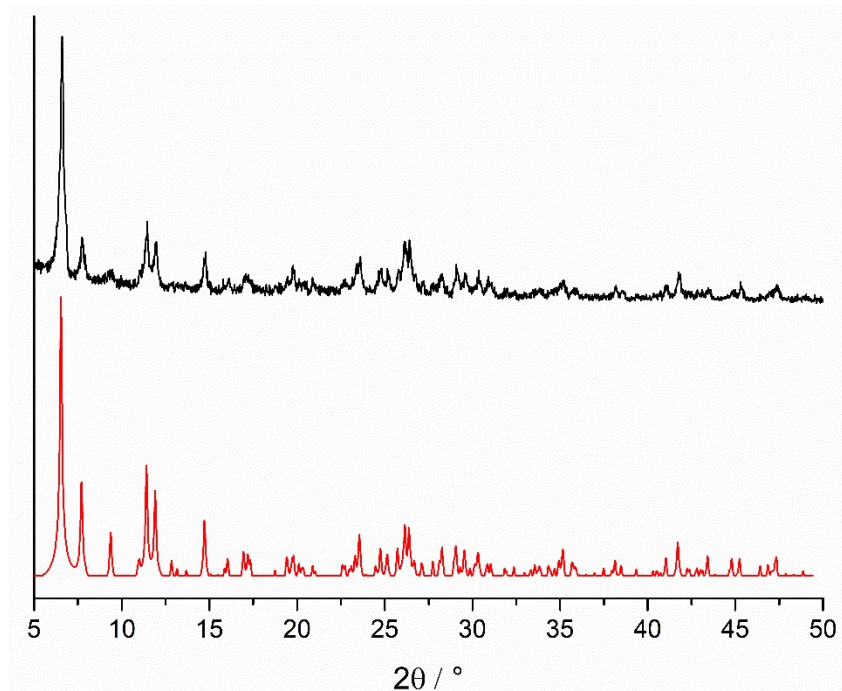


Figure S1. Calculated (red line) and experimental (black line) PXRD patterns of **2,3-ampV₁₀**. Main peaks in the experimental diffractogram are located at 6.6, 7.7, 11.5, 12.0, 14.8, 17.2, 19.7, 23.6, 24.8, 26.1, 28.2, 29.1 and 30.3° 2θ.

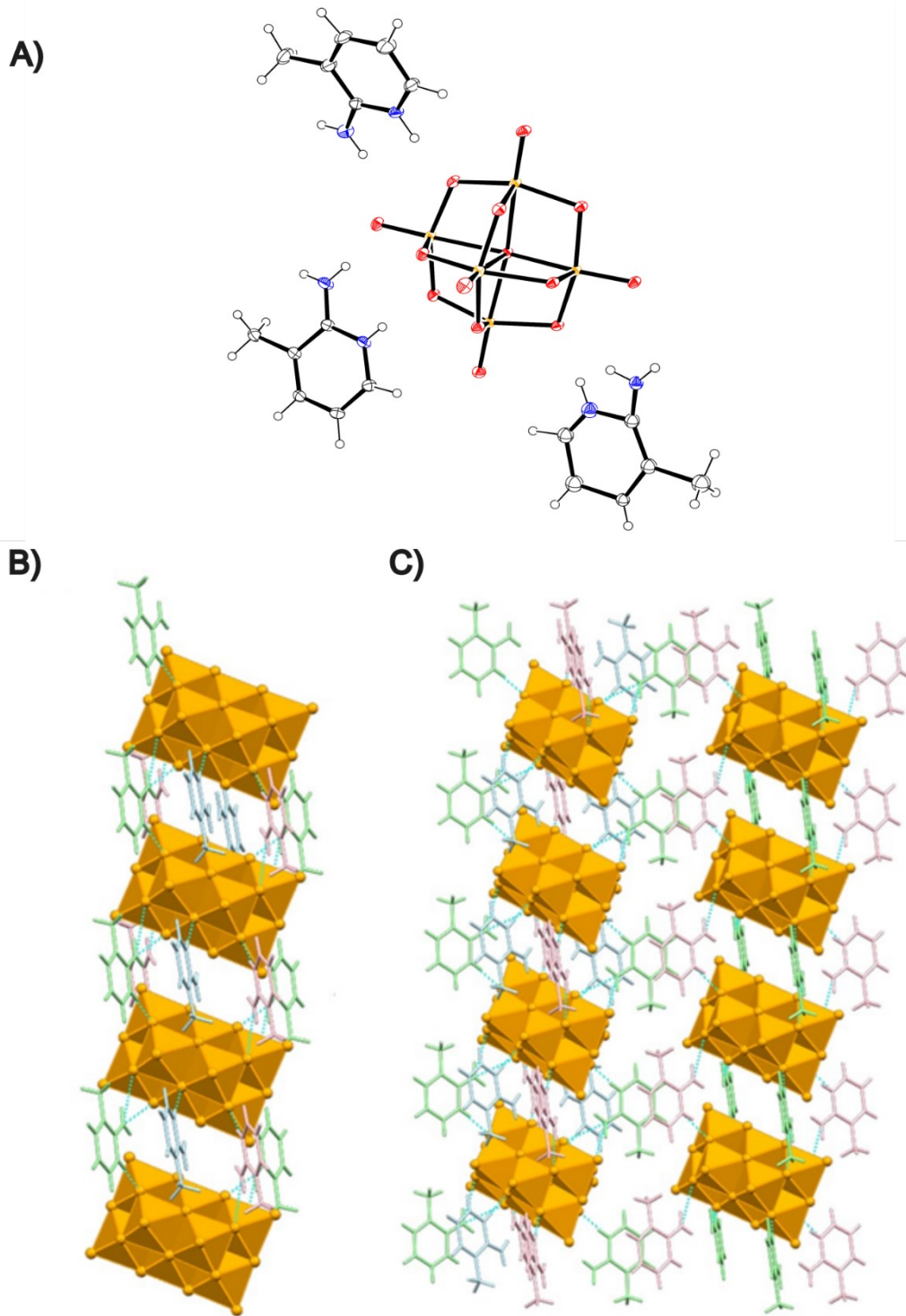


Figure S2. A) ORTEP view of the asymmetric unit of **2,3-ampV₁₀**. Ellipsoid probability 35%, for the disordered 2-amino-3-methylpyridinium cation just the model with the bigger occupancy factor is reported. B) Chain formed by the 2,3-ampH⁺ cation and V₁₀ anions interactions in **2,3-ampV₁₀** (view along the *b* axis). C) 2,3-ampH⁺ cation and V₁₀ anions network (view along the *b* axis). Color scheme: V = yellow, O = red, N = blue.

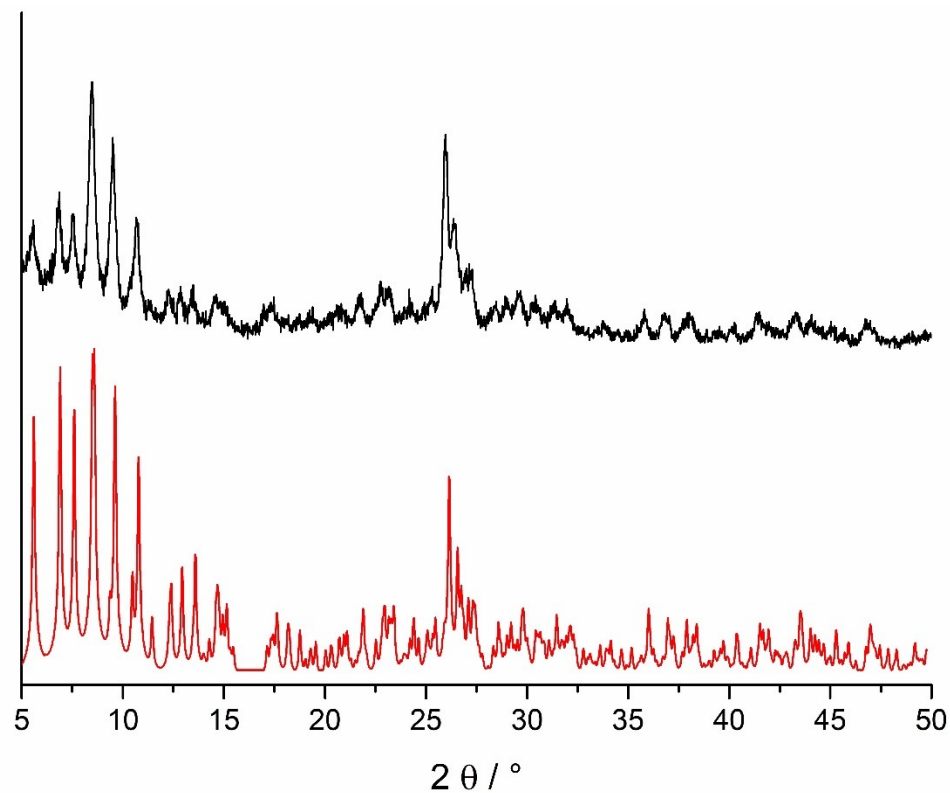


Figure S3. Calculated (red line) and experimental (black line) PXRD patterns of **MBV₁₀**. Main peaks in the experimental diffractogram are located at 5.6, 6.9, 7.5, 8.5, 9.5, 10.6, 26, 26.4, and 27.1° in 2θ.

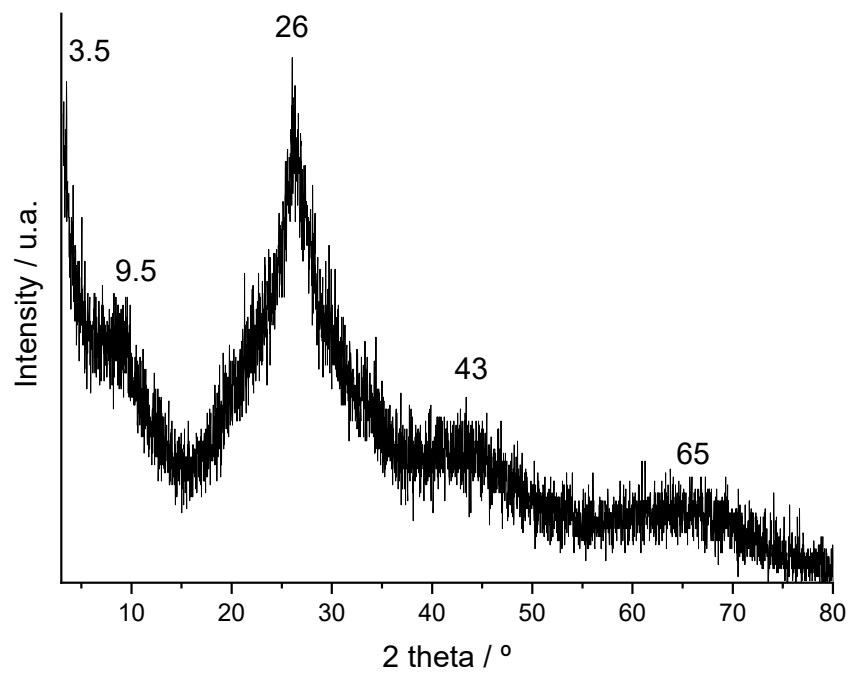


Figure S4. PXRD pattern of **ATV₁₀**.

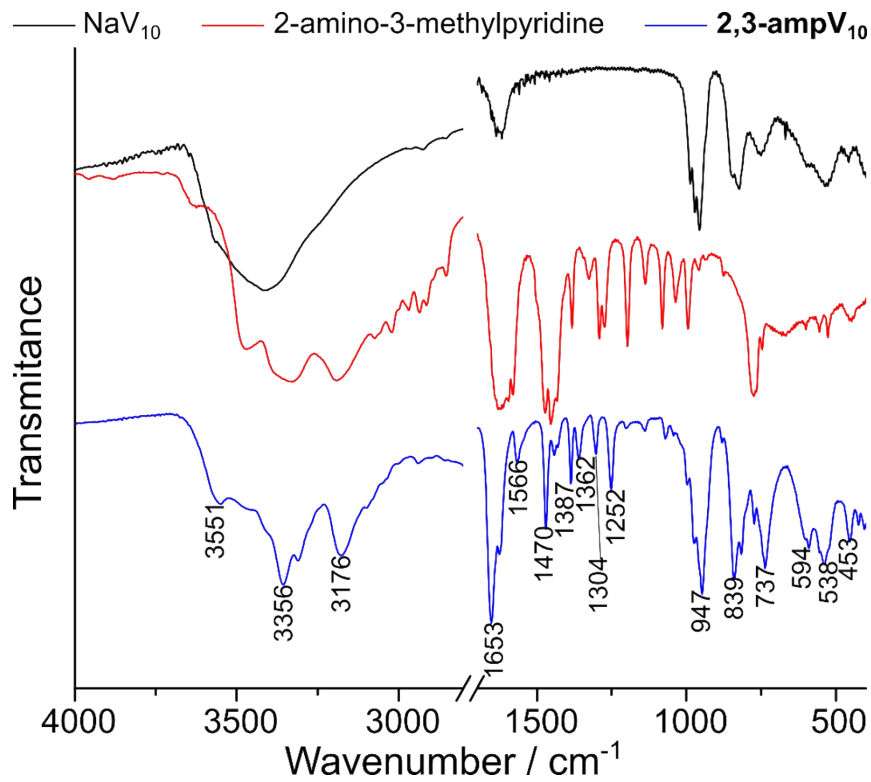


Figure S5. Infrared absorption spectrum of $(2,3\text{-ampH})_6[\text{V}_{10}\text{O}_{28}]\cdot 4\text{H}_2\text{O}$ (**2,3-ampV₁₀**) as compared to its starting materials.

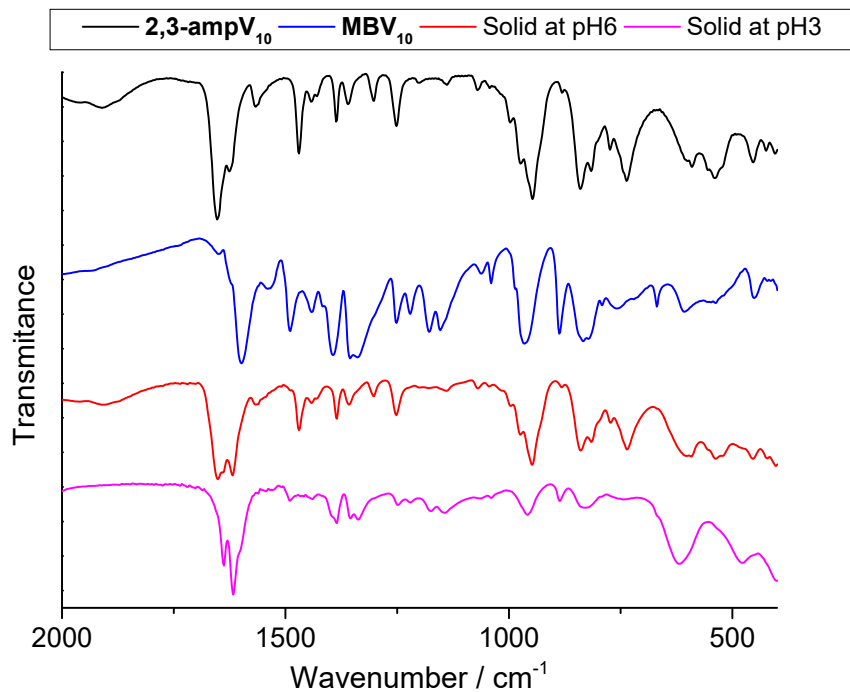


Figure S6. IR spectrum recorded for the remain solids isolated from MB bleaching reactions with **2,3-ampV₁₀**.

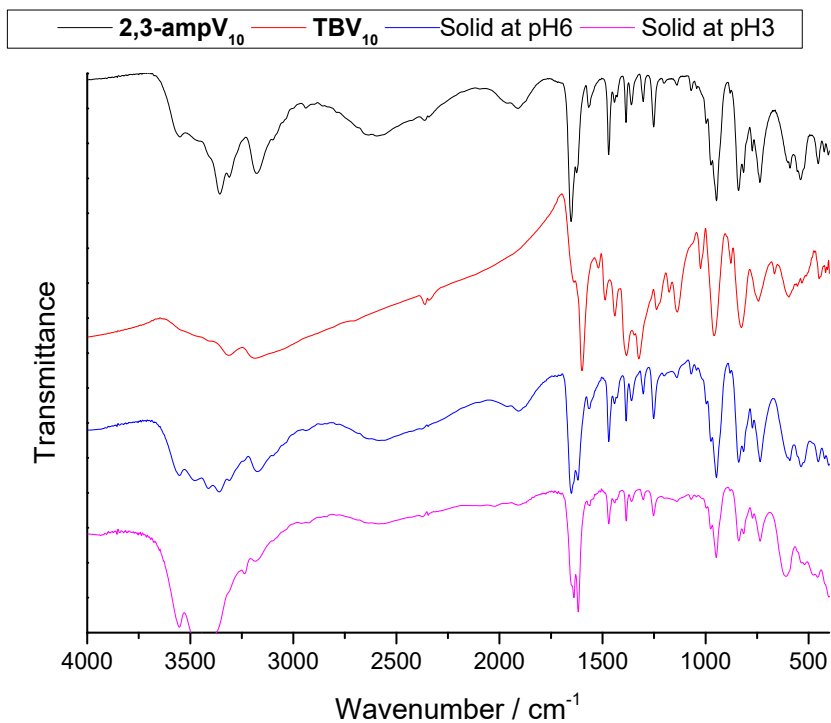


Figure S7. IR spectrum recorded for the solids isolated from TB bleaching reactions with **2,3-ampV₁₀**.

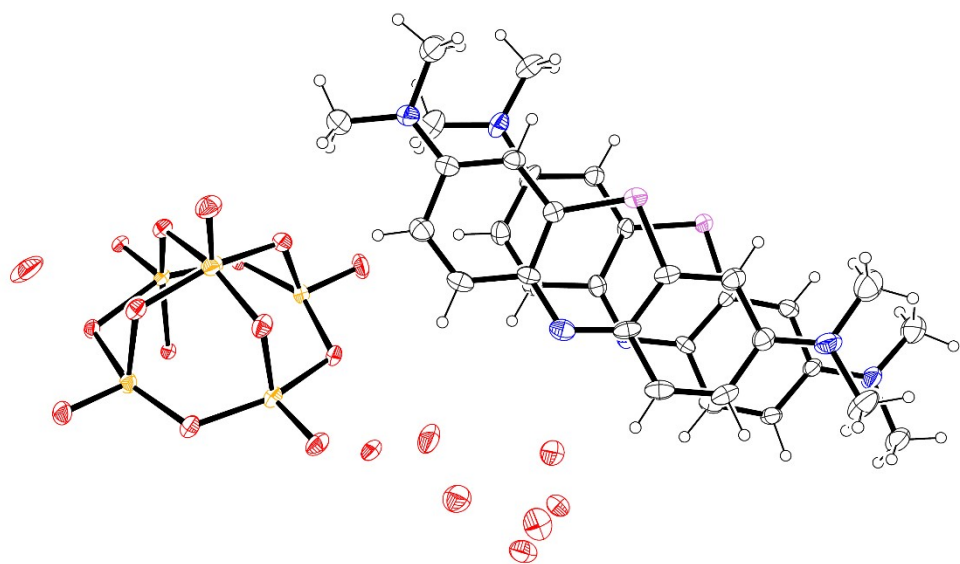


Figure S8. ORTEP view of the asymmetric unit of **MBV₁₀**. Ellipsoid probability 30%. Color scheme: V = yellow, O = red, N = blue and S = purple.

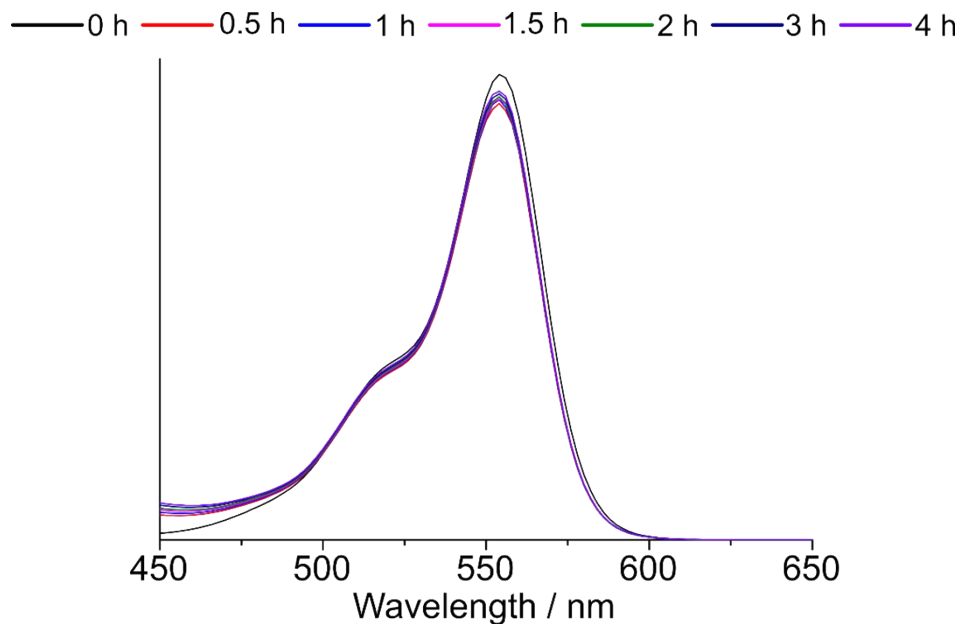


Figure S9. Electronic spectra registered for the supernatants of the bleaching reactions using 10 mg of **2,3-ampV₁₀** in 10 mg L⁻¹ aqueous solution of RB in time.

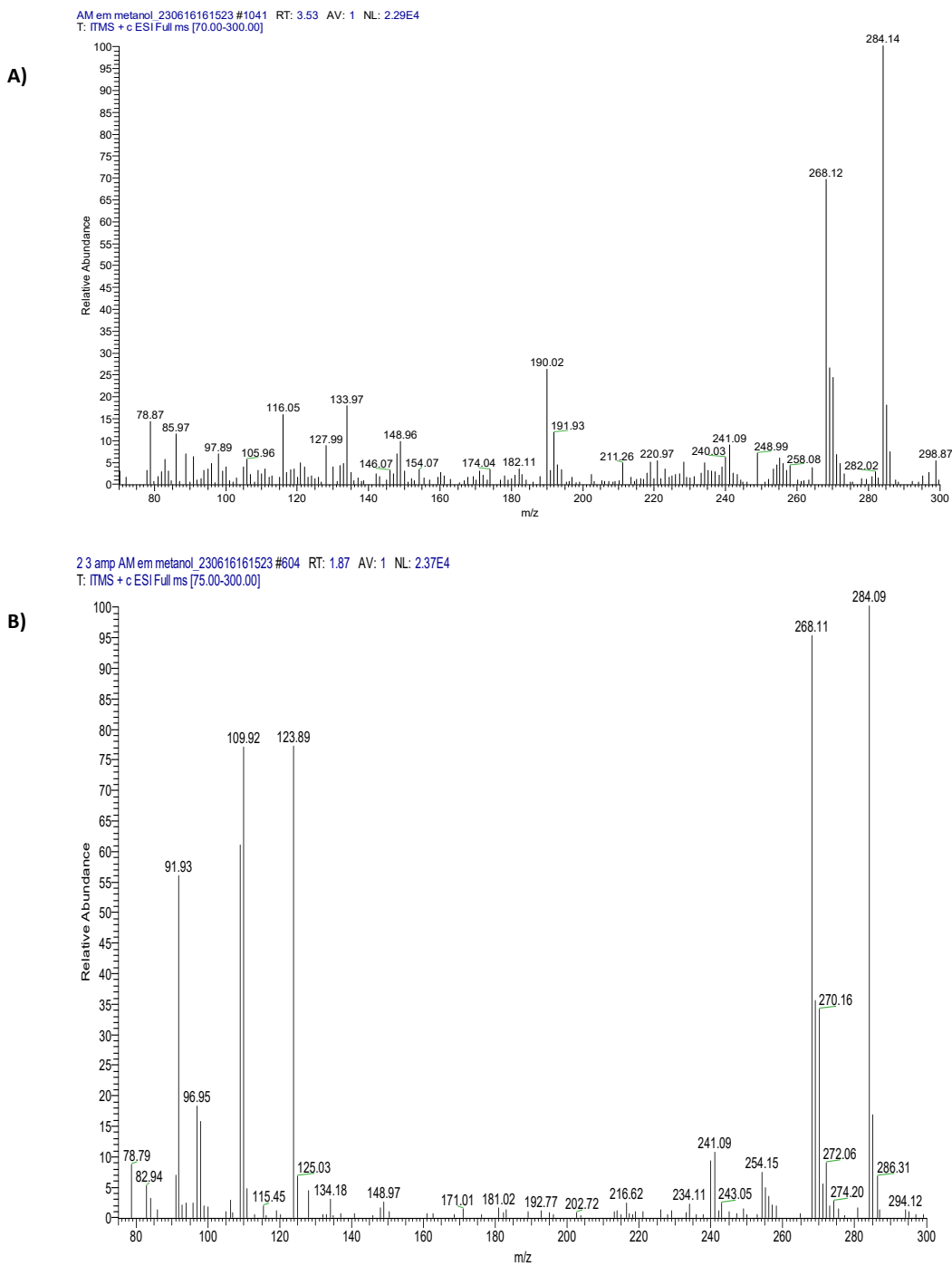


Figure S10. ESI-MS scan of MB (10 mg L^{-1}) in positive mode: **A)** before and **B)** after the reaction with 10 mg of $2,3\text{-ampV}_{10}$.

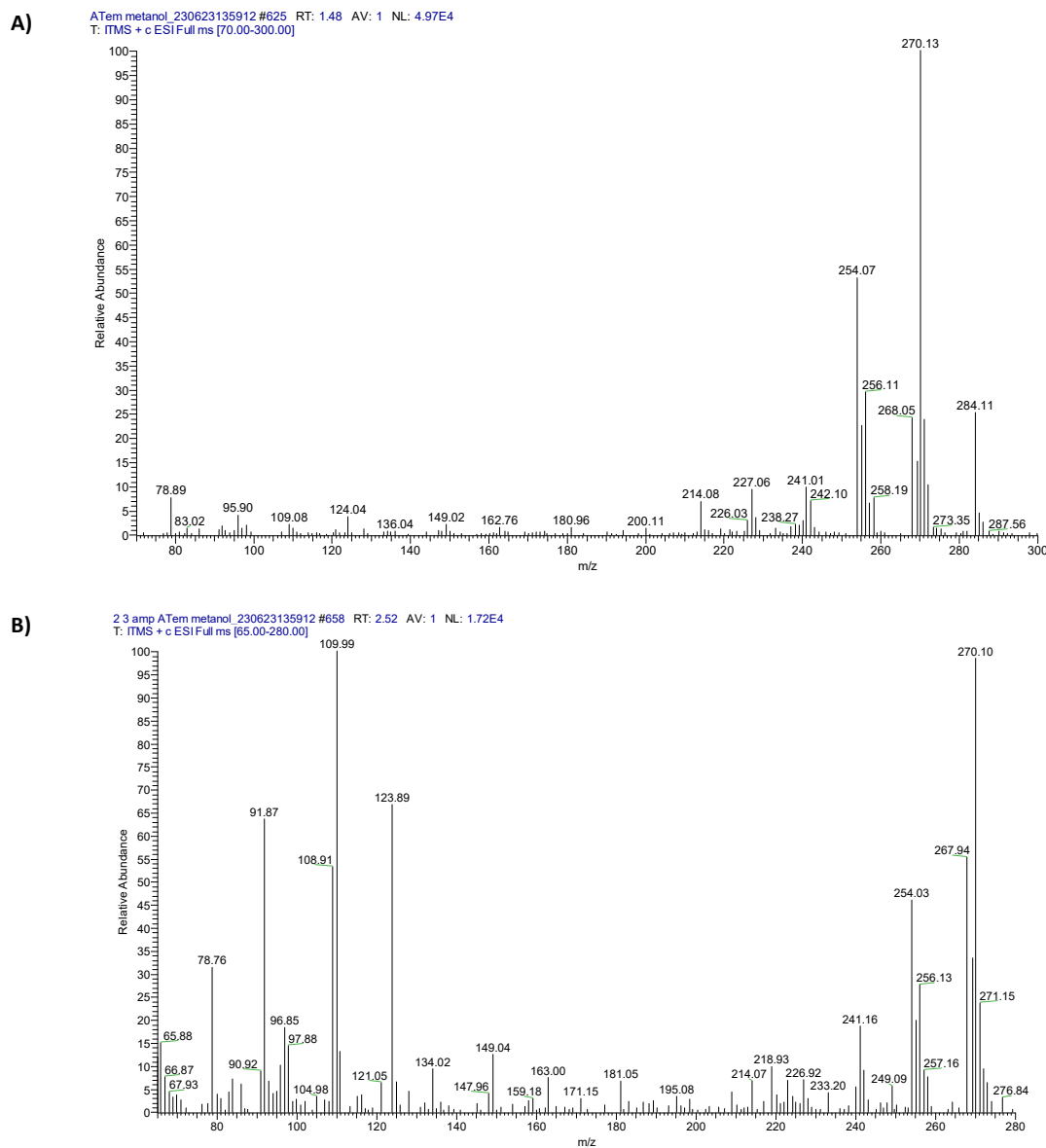


Figure S11. ESI-MS scan of TB (10 mg L^{-1}) in positive mode: **A)** before and **B)** after the reaction with $10 \text{ mg } \mathbf{2,3\text{-ampV}_{10}}$.

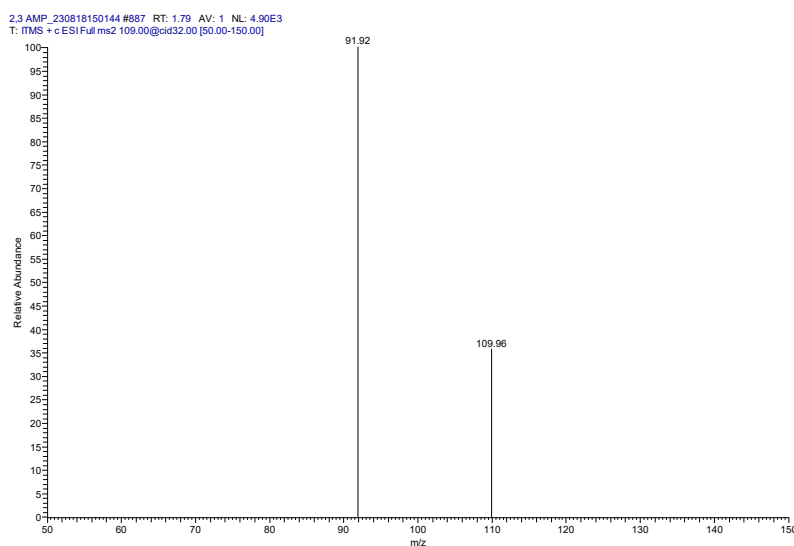


Figure S12. ESI-MS scan of 2-amino-3-methylpyridine in methanol in positive mode. The mass spectra showed peaks at m/z 109.9 that corresponded to the protonated form of $2,3\text{-ampH}^+$. The peak at m/z 91.9 may correspond to C_6NH_6^+ .

References

1. H. Naslajian, M. Amini, S. M. F. Farnia, A. Sheykhi, O. Şahin and O. Z. Yeşilel, *Journal of Coordination Chemistry*, 2017, **70**, 2940-2949.
2. C. Yuan, L. Lu, M. Zhu, Q. Ma and Y. Wu, *Acta Crystallographica Section E*, 2009, **65**, m267-m268.
3. Y. Gong, C. Hu, H. Li, W. Tang, K. Huang and W. Hou, *Journal of Molecular Structure*, 2006, **784**, 228-238.
4. L. Bartošová, Z. Padělková, E. Rakovský and P. Schwendt, *Polyhedron*, 2012, **31**, 565-569.
5. S. R. Amanchi and S. K. Das, *Frontiers in Chemistry*, 2018, **6**, 469.
6. A. S. Rao, T. Arumuganathan, V. Shivaiah and S. K. Das, *Journal of Chemical Sciences*, 2011, **123**, 229-239.
7. E. Sánchez-Lara, B. Martínez-Valencia, N. D. Corona-Motolinia, B. L. Sanchez-Gaytan, M. E. Castro, S. Bernès, M. A. Méndez-Rojas, F. J. Meléndez-Bustamante and E. González-Vergara, *New Journal of Chemistry*, 2019, **43**, 17746-17755.
8. B. Wu, X. Xu, K. Chen, Z. Xiao and P. Wu, 2015, *Zeitschrift für Kristallographie - New Crystal Structures*, **230**, 353-355.
9. E. Sánchez-Lara, A. Pérez-Benítez, S. Treviño, A. Mendoza, F. J. Meléndez, E. Sánchez-Mora, S. Bernès and E. González-Vergara, *Crystals*, 2016, **6**, 65.
10. E. Sánchez-Lara, I. Sánchez-Lombardo, A. Pérez-Benítez, Á. Mendoza, M. Flores-Álamo and E. G. Vergara, *Journal of Cluster Science*, 2015, **26**, 901-912.
11. R. Dridi, Z. Abdelkafi-Koubaa, N. Srairi-Abid, B. Socha and M. F. Zid, *Journal of Inorganic Biochemistry*, 2024, **255**, 112533.
12. R. L. Frost, K. L. Erickson, M. L. Weier and O. Carmody, *Spectrochimica Acta Part A: Molecular and Biomolecular Spectroscopy*, 2005, **61**, 829-834.
13. N. Sundaraganesan, C. Meganathan and M. Kurt, *Journal of Molecular Structure*, 2008, **891**, 284-291.
14. O. V. Ovchinnikov, A. V. Evtukhova, T. S. Kondratenko, M. S. Smirnov, V. Y. Khokhlov and O. V. Erina, *Vibrational Spectroscopy*, 2016, **86**, 181-189.
15. A. Belcaid, B. H. Beakou, S. Bouhsina and A. Anouar, *Biomass Conversion and Biorefinery*, 2024, **14**, 7783-7806.
16. K. Thenmozhi and S. Sriman Narayanan, *Analytical and bioanalytical chemistry*, 2007, **387**, 1075-1082.
17. M. A. Nasher, M. I. Youssif, N. A. El-Ghamaz and H. M. Zeyada, *Optik*, 2019, **178**, 532-543.